Coordination of the leucine-sensing Rag GTPase cycle by leucyl-tRNA synthetase in the mTORC1 signaling pathway

Minji Lee[a,1], Jong Hyun Kim[b,1], Ina Yoon[b], Chulho Lee[a,c], Mohammad Fallahi Sichani[d], Jong Soon Kang[e], Jeonghyun Kang[f], Min Guo[d], Kang Young Lee[f], Gyoonhee Han[a,c], Sunghoon Kim[b,g,2], and Jung Min Han[a,h,2]

[a]Department of Integrated OMICS for Biomedical Science, Yonsei University, Seoul 03722, South Korea; [b]Medicinal Bioconvergence Research Center, College of Pharmacy, Seoul National University, Seoul 08826, South Korea; [c]Translational Research Center for Protein Function Control, Department of Biotechnology, Yonsei University, Seoul 03722, South Korea; [d]Department of Cancer Biology, The Scripps Research Institute, Scripps Florida, Jupiter, FL 33458; [e]Bioevaluation Center, Korea Research Institute of Bioscience and Biotechnology, Ochang, Chungbuk 28116, South Korea; [f]Department of Surgery, College of Medicine, Severance Hospital, Yonsei University, Seoul 03722, South Korea; [g]Department of Molecular Medicine and Biopharmaceutical Sciences, Graduate School of Convergence Science and Technology, Seoul National University, Seoul 08826, South Korea; and [h]College of Pharmacy, Yonsei University, Incheon 21983, South Korea

Edited by Paul Schimmel, The Scripps Research Institute, Jupiter, FL, and approved May 2, 2018 (received for review January 23, 2018)

A protein synthesis enzyme, leucyl-tRNA synthetase (LRS), serves as a leucine sensor for the mechanistic target of rapamycin complex 1 (mTORC1), which is a central effector for protein synthesis, metabolism, autophagy, and cell growth. However, its significance in mTORC1 signaling and cancer growth and its functional relationship with other suggested leucine signal mediators are not well-understood. Here we show the kinetics of the Rag GTPase cycle during leucine signaling and that LRS serves as an initiating "ON" switch via GTP hydrolysis of RagD that drives the entire Rag GTPase cycle, whereas Sestrin2 functions as an "OFF" switch by controlling GTP hydrolysis of RagB in the Rag GTPase–mTORC1 axis. The LRS–RagD axis showed a positive correlation with mTORC1 activity in cancer tissues and cells. The GTP–GDP cycle of the RagD–RagB pair, rather than the RagC–RagA pair, is critical for leucine-induced mTORC1 activation. The active RagD–RagB pair can overcome the absence of the RagC–RagA pair, but the opposite is not the case. This work suggests that the GTPase cycle of RagD–RagB coordinated by LRS and Sestrin2 is critical for controlling mTORC1 activation, and thus will extend the current understanding of the amino acid-sensing mechanism.

leucyl-tRNA synthetase | Rag GTPase | mTORC1 | GTPase-activating protein | Sestrin2

Mechanistic target of rapamycin complex 1 (mTORC1) coordinates several upstream signals such as growth factors, intracellular amino acid availability, and energy status to regulate protein synthesis, autophagy, and cell growth (1–3), and is implicated in many human diseases including cancer, epilepsy, obesity, and diabetes (4–6). Rag GTPases have been shown to be amino acid-responsive mediators of the mTORC1 pathway (7, 8). Mammals express four Rag GTPases—RagA, RagB, RagC, and RagD (9, 10). Rag GTPases form obligate heterodimers of either RagA–RagC or RagB–RagD to mediate amino acid-induced mTORC1 activation (7–10). Amino acids induce the translocation of mTORC1 to the lysosome, where Rag heterodimers containing GTP-bound RagB interact with mTORC1 (11). Guanine nucleotide exchange factors (GEFs) regulate small GTPases. GEFs promote GDP-to-GTP exchange; GTPase-activating protein (GAP), which stimulates GTP hydrolysis; and guanine nucleotide dissociation inhibitor (GDI), which forms a stable complex with small GTPases (12). However, how the GTP–GDP cycle of Rag GTPases is concertedly regulated in leucine signaling is not understood.

Regulators of the Rag GTPases have recently been identified. Leucyl-tRNA synthetase (LRS) was first identified as a leucine sensor for mTORC1 by functioning as a GAP for RagD (13). Cdc60, a yeast LRS, interacts with the Rag GTPase Gtr1 of the yeast EGO complex in a leucine-dependent manner and mediates leucine signaling to TORC1 (14). Recently, the novel mTORC1 inhibitor BC-LI-0186 was shown to specifically block the leucine-sensing function of LRS by inhibiting its interaction with RagD (15). Two protein complexes, GATOR1 (NPRL2, NPRL3, and DEPDC5) and GATOR2 (Milos, WDR24, WDR59, SEHL1L, and SEC13), are also known to be critical regulators of amino acid signaling to mTORC1 (16). GATOR1 works as a GAP for RagA–RagB, which is controlled by GATOR2 (16). Sestrin1 and Sestrin2, which are p53 target genes (17, 18), are negative regulators of mTOR (19). Sestrin2 was recently reported to regulate mTORC1 activity through the functions of RagA–RagB GDI or GAP (20, 21). In the latter case, Sestrin2 binds to leucine and regulates the GATOR2–GATOR1 pathway (22, 23). The Ragulator complex, which comprises five components, LAMTOR1, LAMTOR2, LAMTOR3, LAMTOR4, and LAMTOR5 (24), controls the lysosomal localization of the Rag heterodimer (11). Ragulator has a preference for GDP-bound RagA and RagB and possesses GEF

Significance

LRS, an enzyme involved in protein synthesis, and Sestrin2, a stress-induced metabolic protein, are suggested to function as leucine sensors for the mTORC1 pathway, a central regulator of cell metabolism, growth, proliferation, and survival. The Rag GTPase cycle regulates mTORC1; however, regulators of the Rag GTPase cycle and their coordination remain unknown. We show the dynamics of the RagD–RagB GTPase cycle during leucine signaling and describe contrasting yet complementary roles for LRS and Sestrin2 in the Rag GTPase–mTORC1 pathway, functioning as "ON" and "OFF" switches, respectively. Our results extend the current view of amino acid sensing by mTORC1 and will be invaluable for the development of novel approaches to combat mTORC1-related human diseases such as cancer.

Author contributions: M.L., J.H.K., M.G., G.H., and J.M.H. designed research; M.L., J.H.K., J.S.K., J.K., and J.M.H. performed research; K.Y.L. contributed new reagents/analytic tools; M.L., J.H.K., I.Y., C.L., M.F.S., J.S.K., J.K., M.G., K.Y.L., and J.M.H. analyzed data; S.K. and J.M.H. supervised the study; and M.L., J.H.K., S.K., and J.M.H. wrote the paper.

Conflict of interest statement: Paul Schimmel and M.G. have coauthored papers, most recently in 2014.

This article is a PNAS Direct Submission.

[1]M.L. and J.H.K. contributed equally to this work.

[2]To whom correspondence may be addressed. Email: sungkim@snu.ac.kr or jhan74@yonsei.ac.kr.

This article contains supporting information online at www.pnas.org/lookup/suppl/doi:10.1073/pnas.1801287115/-/DCSupplemental.

Published online May 21, 2018.

activity toward RagA and RagB (24). Despite considerable progress in understanding how Rag GTPase functions in leucine signaling to mTORC1, the functional relationship among the suggested leucine sensors and how their roles are coordinated through Rag GTPases are not yet understood. Here we show that the heterodimer of Rag GTPases consisting of RagD and RagB is critical for leucine signaling to mTORC1. Upon leucine stimulation, GTP hydrolysis of RagD, which is mediated by LRS, drives the entire Rag GTPase cycle, whereas GTP loading of RagB, which is controlled by the Ragulator complex and Sestrin2, activates mTORC1. We validated the functional significance of the LRS–Rag GTPase–mTORC1 signaling axis by pathological analysis of colon cancer tissues and cells.

Results

Positive Correlation of LRS and mTORC1 Signaling in Cancer Tissues and Cells. Since mTORC1 is hyperactivated in many human cancers (25, 26), we analyzed the relationship of LRS expression to that of mTORC1 pathway genes in cancer, using the Oncomine cancer profiling database and The Cancer Genome Atlas (TCGA). The Oncomine database indicated that gene expression of *LARS* was increased in colon adenoma (Fig. 1*A*), colon carcinoma (Fig. 1*B*), rectosigmoid adenocarcinoma (Fig. 1*C*), floor of the mouth carcinoma (*SI Appendix*, Fig. S1*A*), skin squamous cell carcinoma (*SI Appendix*, Fig. S1*B*), and acute myeloid leukemia (*SI Appendix*, Fig. S1*C*) compared with the corresponding normal tissues. In contrast, *SESN2* expression was down-regulated in colon adenoma (*SI Appendix*, Fig. S1*D*), colon carcinoma (*SI Appendix*, Fig. S1*E*), and T cell lymphoma (*SI Appendix*, Fig. S1*F*). In searching TCGA database, we also found that gene expression of *LARS* and *RHEB*, but not *MTOR*, *RRAGA*, *RRAGC*, and *RRAGD*, was increased in primary tumor tissues compared with normal tissues (Fig. 1 *D* and *E*). We next performed immunohistochemistry (IHC) staining to detect levels of LRS in human colorectal cancer (CRC) and adjacent normal tissues. We found that LRS levels were higher in tumors compared with the matching normal tissues (Fig. 1*F*). Remarkably, in 95 of the total 117 CRC cases (81.2%), LRS levels were higher in tumors than in the matching normal tissues (Fig. 1*G*). We further examined the relationship between LRS levels and mTORC1 activity by IHC staining of LRS and p-S6 in tumors and the matched normal tissues. In 79 of 117 cases (67.5%) (34 cases of low LRS and low p-S6 and 45 cases of high LRS and high p-S6), LRS levels showed positive correlation with p-S6 staining (Fig. 1 *H* and *I*). We also

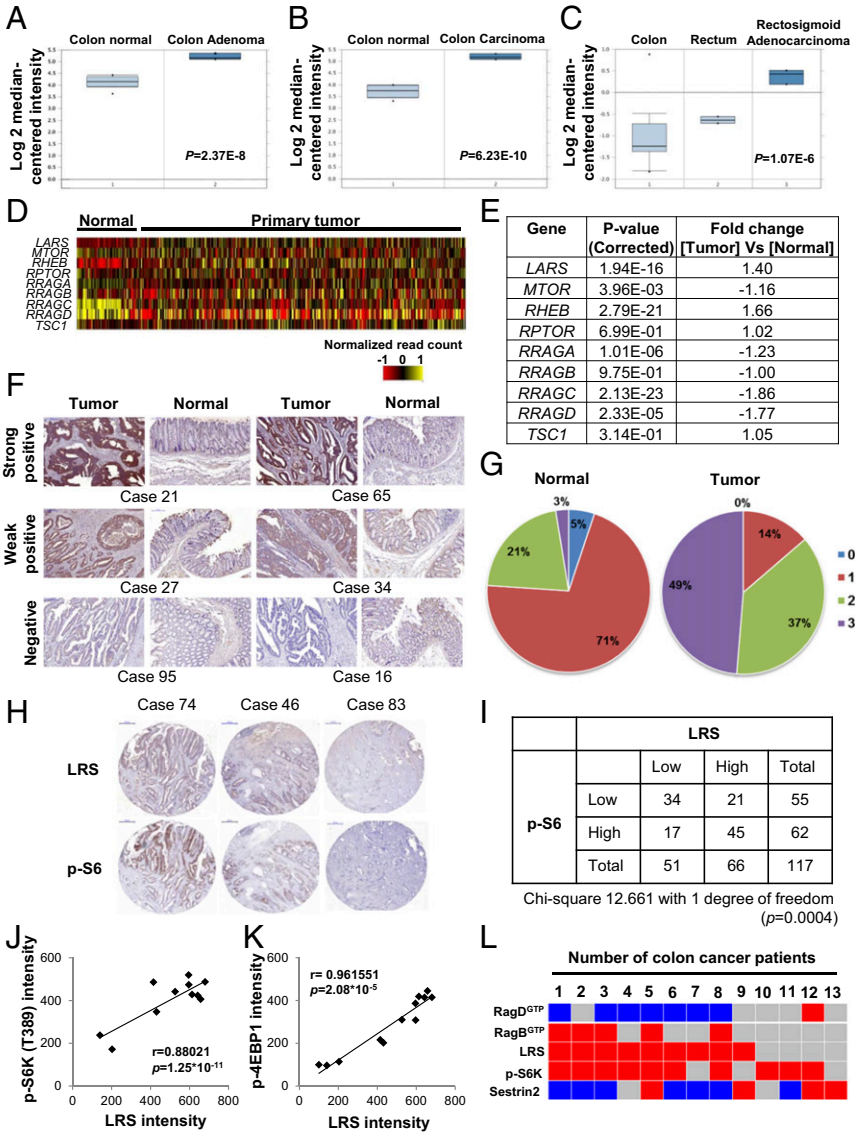

Gene	P-value (Corrected)	Fold change [Tumor] Vs [Normal]
LARS	1.94E-16	1.40
MTOR	3.96E-03	-1.16
RHEB	2.79E-21	1.66
RPTOR	6.99E-01	1.02
RRAGA	1.01E-06	-1.23
RRAGB	9.75E-01	-1.00
RRAGC	2.13E-23	-1.86
RRAGD	2.33E-05	-1.77
TSC1	3.14E-01	1.05

		LRS		
		Low	High	Total
p-S6	Low	34	21	55
	High	17	45	62
	Total	51	66	117

Chi-square 12.661 with 1 degree of freedom (p=0.0004)

Fig. 1. Correlation of LRS expression with hyperactive mTORC1 in cancer cells. (*A*–*C*) Boxplots showing the expression level of *LARS* in colon adenoma (*A*; $P = 2.37E^{-8}$), colon carcinoma (*B*; $P = 6.23E^{-10}$), and rectosigmoid adenocarcinoma (*C*; $P = 1.07E^{-6}$). *LARS* data were extracted from the Oncomine database and expressed as log2 median-centered intensity. (*D*) Heatmap of gene expression of *LARS* and *MTOR* pathway genes in TCGA dataset ($n = 433$). (*E*) Fold change of the selected genes *LARS*, *MTOR*, *RHEB*, *RPTOR*, *RRAGA*, *RRAGB*, *RRAGC*, *RRAGD*, and *TSC1* in mTOR pathway genes. (*F*) Immunostaining of LRS in colorectal tumor and normal tissues with anti-LRS antibody. Representative images for strong, weak, or negative LRS staining are shown. Case numbers indicate different patients. (*G*) Intensity scores of LRS staining in colorectal tumor or normal tissues are shown as circle graphs. Scores 3 (purple) or 2 (green), 1 (red), and 0 (blue) stand for strong, weak, and negative LRS staining, respectively ($n = 117$). (*H*) Consecutive tissue images were stained for LRS or S6 phosphorylation. Representative images for strong, weak, or negative LRS and S6 phosphorylation staining are shown. (Scale bar, 100 μm.) (*I*) Total number is shown as a table with low and high staining for LRS or S6 phosphorylation. (*J*) Correlation between cellular levels of LRS and S6K phosphorylation shown in *SI Appendix*, Fig. S1*G* is displayed as a scatterplot and evaluated by a Pearson correlation coefficient. (*K*) Correlation between cellular levels of LRS and 4E-BP1 phosphorylation shown in *SI Appendix*, Fig. S1*G* is displayed as a scatterplot and evaluated by a Pearson correlation coefficient. (*L*) Heatmap of the protein intensity ratio of tumor/normal tissues shown in *SI Appendix*, Fig. S1*J*. Blue indicates the ratio of tumor/normal tissues is below 0.8. Red indicates the ratio is higher than 1.2, and gray indicates the ratio is between 0.8 and 1.2.

analyzed the cellular levels of mTORC1 pathway-related factors, including LRS in 12 colon cancer cell lines compared with colon normal epithelial cells. The LRS levels were higher in all of the tested colon cancer cells than in normal epithelial cells (*SI Appendix*, Fig. S1*G*) and showed a positive correlation with phosphorylation of S6K (Fig. 1*J*) and 4E-BP1 (Fig. 1*K*), both of which are known substrates of mTORC1. In addition, overexpression of LRS showed a positive correlation with mTORC1 in several types of cancer, including breast cancer, ovarian cancer, glioblastoma multiform, and pancreatic cancer (*SI Appendix*, Fig. S1 *H* and *I*). In 7 of 13 fresh biopsy specimens from CRC patients (53.85%), LRS levels showed a reverse correlation with $RagD^{GTP}$ (high LRS/low $RagD^{GTP}$). In seven cases (53.85%), LRS levels showed a positive correlation with p-S6K levels (high LRS and high p-S6K). In four cases, high LRS levels showed a positive correlation not only with high p-S6K levels but also with low $RagD^{GTP}$ and high $RagB^{GTP}$ (Fig. 1*L* and *SI Appendix*, Fig. S1*J*). These results suggest that simultaneous increases in LRS levels and mTORC1 activities are clinically associated with human colon cancer tissues and cells.

Distinct Roles of LRS and Sestrin2 in the Control of the Rag GTPase–mTORC1 Axis. We investigated the GTP–GDP status of RagD and RagB upon leucine stimulation. Leucine treatment induced GTP hydrolysis of RagD and GTP loading of RagB (Fig. 2*A*) but did not affect the GTP–GDP status of endogenous ARF1, as previously reported (27). To understand the systemic changes in Rag GTPases, we also analyzed the leucine-dependent changes in Rag GTPases using a GTP-conjugated bead pull-down method. Agarose beads conjugated to GTP, but not m^7GTP, specifically precipitated the GTP-bound form of RagD (RagD Q121L) (*SI Appendix*, Fig. S2*A*). Precipitation of the GTP-bound form of RagD, as well as endogenous GTP-bound ARF1 ($ARF1^{GTP}$), was suppressed by GTPγS but not by GDPβS, indicating the specificity of GTP binding to small GTPases (Fig. 2*B* and *SI Appendix*, Fig. S2*B*). When the GTP- or GDP-bound form of Rag GTPases was cotransfected into cells, only the GTP-bound forms of Rag GTPases were precipitated, supporting the specificity of the GTP-agarose pull-down assay (*SI Appendix*, Fig. S2*C*). Next, we investigated the GTP–GDP status of endogenous RagD and RagB upon leucine stimulation. Whereas the GTP–GDP status of endogenous ARF1 was unaffected by leucine treatment, the level of GTP-bound RagD ($RagD^{GTP}$) was decreased and level of GTP-bound RagB ($RagB^{GTP}$) was increased (Fig. 2*B*), further validating the GTP-agarose pull-down assay.

We then investigated the functional relationship between LRS and other regulators of Rag GTPases. LRS binds to $RagD^{GTP}$ and functions as a GAP for RagD (13). The Ragulator complex is a GEF for RagA and RagB (24). Sestrin2 has been suggested to regulate RagA–RagB GAP activity via the GATOR2–GATOR1 pathway (16, 21, 23, 28). GATOR1 inactivates $RagA^{GTP}$ and $RagB^{GTP}$ that are required for mTORC1 activation (16). Thus, we first examined the differential binding of these regulators with HA-tagged Rag GTPases by immunoprecipitation. LRS, but not other tRNA synthetases such as isoleucyl-tRNA synthetase (IRS) and glutamyl-prolyl-tRNA synthetase (EPRS), specifically bound to $RagD^{GTP}$ (Fig. 2*C*). LAMTOR2 and LAMTOR3 (components of the Ragulator complex) bound to $RagB^{GDP}$ and $RagA^{GDP}$, while DEPDC5 (a component of the GATOR1 complex) bound to $RagB^{GTP}$ and $RagA^{GTP}$. However, WDR24 and Sec13 (components of the GATOR2 complex) and Sestrin2 were not detected in any of the Rag GTPase immunoprecipitates (Fig. 2*C*). These results support previous reports regarding the role of LRS, Ragulator, and GATOR1 in regulating Rag GTPases.

Next, we compared the roles of two leucine sensors, LRS and Sestrin2, in the control of Rag GTPases. LRS knockdown suppressed leucine-induced changes in $RagD^{GTP}$ and $RagB^{GTP}$, and mTORC1 activation. In contrast, Sestrin1/2 knockdown increased $RagB^{GTP}$ and activated mTORC1 without affecting the leucine-induced change of $RagD^{GTP}$ (Fig. 2*D*). LRS overexpression decreased $RagD^{GTP}$ and increased $RagB^{GTP}$, resulting in mTORC1 activation even in the absence of leucine. In contrast, Sestrin2 overexpression specifically decreased $RagB^{GTP}$ and mTORC1 activation without affecting leucine-induced change in $RagD^{GTP}$ (Fig. 2*E*), suggesting that LRS and Sestrin2 play distinct roles in regulating Rag GTPases.

Since treatment of BC-LI-0186, which is a novel LRS-binding compound and an inhibitor of LRS–RagD binding, arrested the Rag GTPase cycle and the deprivation of BC-LI-0186 reactivated this cycle (15), we used it as a tool to monitor kinetic changes in Rag GTPases resulting from varying levels of LRS or Sestrin2. We monitored the kinetic changes of $RagD^{GTP}$ and $RagB^{GTP}$ after depriving cells of BC-LI-0186 under conditions of overexpression and knockdown of LRS or Sestrin2. Levels of $RagD^{GTP}$ were decreased and $RagB^{GTP}$ increased by the up-regulation of LRS (Fig. 2 *F* and *G* and *SI Appendix*, Fig. S2*D*), and the converse was observed by down-regulation of LRS (Fig. 2 *H* and *I* and *SI Appendix*, Fig. S2*E*). The LRS-dependent conversion of $RagB^{GTP}$ also showed a positive correlation with S6K phosphorylation. However, the changes in Sestrin2 levels only affected $RagB^{GTP}$ levels. $RagB^{GTP}$ formation was reduced by an increase in Sestrin2 levels but enhanced by Sestrin1/2 suppression with little change to $RagD^{GTP}$ (Fig. 2 *J–M* and *SI Appendix*, Fig. S2 *F* and *G*). Together, these results suggest that LRS and Sestrin2 play distinct roles in the control of Rag GTPases.

Kinetics of the Rag GTPase Cycle During Leucine Signaling. To understand the exact roles of LRS and Sestrin2 in the control of Rag GTPases, we analyzed the kinetics of the Rag GTPase cycle in response to varying levels of amino acids or leucine. First, we monitored the molecular behavior of endogenous Rag GTPases under amino acid/leucine supplementation or deprivation. Under amino acid–leucine deprivation conditions, RagD and RagC were initially GTP-loaded whereas RagB and RagA were GDP-loaded (Fig. 3 *A* and *B* and *SI Appendix*, Fig. S3 *A* and *B*). However, upon amino acid or leucine supplementation, RagD and RagC became GDP-loaded and RagB and RagA became GTP-loaded over time (Fig. 3 *A* and *B* and *SI Appendix*, Fig. S3 *A* and *B*). Conversely, under leucine-containing conditions, RagD and RagC were initially GDP-loaded and RagB and RagA were GTP-loaded. Upon leucine deprivation, RagD and RagC became GTP-loaded and RagB and RagA became GDP-loaded over time (Fig. 3 *C* and *D* and *SI Appendix*, Fig. S3 *C* and *D*). These results indicate that the kinetic change of the Rag heterodimer during leucine signaling is as follows: ($RagD^{GTP}$–$RagB^{GDP}$ and $RagC^{GTP}$–$RagA^{GDP}$) → ($RagD^{GDP}$–$RagB^{GDP}$ and $RagC^{GDP}$–$RagA^{GDP}$) → ($RagD^{GDP}$–$RagB^{GTP}$ and $RagC^{GDP}$–$RagA^{GTP}$) → ($RagD^{GDP}$–$RagB^{GDP}$ and $RagC^{GDP}$–$RagA^{GDP}$) → ($RagD^{GTP}$–$RagB^{GDP}$ and $RagC^{GTP}$–$RagA^{GDP}$), which led us to propose a model of the Rag GTPase cycle (Fig. 3*E*). It is known that Rag GTPases function as obligate heterodimers to activate mTORC1 (7). However, which heterodimer of Rag GTPases is a key player for mTORC1 activation is unclear. In our model of kinetics, the activation of the RagD–RagB pair (i.e., the loss of $RagD^{GTP}$ and the gain of $RagB^{GTP}$) occurred before that of the RagC–RagA pair (Fig. 3 *A* and *B* and *SI Appendix*, Fig. S3 *A* and *B*). Also, the inactivation of the RagD–RagB pair (i.e., the gain of $RagD^{GTP}$ and the loss of $RagB^{GTP}$) also occurred before that of the RagC–RagA pair (Fig. 3 *C* and *D* and *SI Appendix*, Fig. S3 *C* and *D*). Therefore, the RagD–RagB pair appears to respond to the variation of amino acid or leucine levels more rapidly than the RagC–RagA pair. Moreover, the time course of S6K phosphorylation and GTP binding of eIF2, which mediates the binding of $tRNA_i^{Met}$ to the ribosome and is critical for translation initiation (29), was more closely correlated with

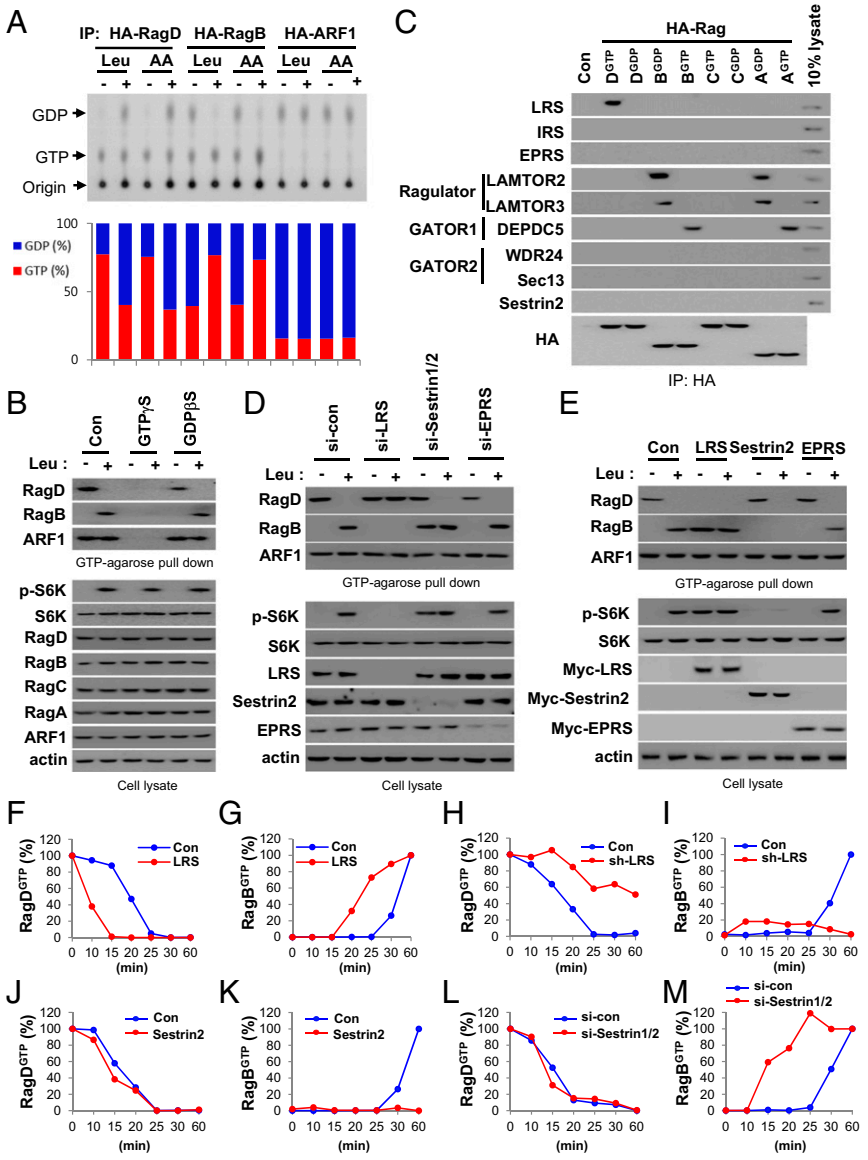

Fig. 2. Distinct roles of LRS and Sestrin2 in the Rag GTPase–mTORC1 axis. (*A*) SW620 cells transfected with HA-RagD^{WT}, RagB^{WT}, or ARF1^{WT} were labeled with 100 μCi/mL [^{32}P]orthophosphate for 8 h, starved of amino acids or leucine for 90 min, and then restimulated with amino acids or leucine for 10 min. The bound nucleotides of the precipitated HA-tagged proteins were eluted and analyzed by TLC (*Upper*). GDP (%) and GTP (%) indicate GDP/(GDP + GTP) × 100 and GTP/(GDP + GTP) × 100, respectively (*Lower*). IP, immunoprecipitation. (*B*) Specificity of the GTP-conjugated agarose bead method. GTPγS or GDPβS (100 μM) was used to confirm the binding specificity of the beads. (*C*) HA-RagD^{GTP} (D^{GTP}, Q121L), RagD^{GDP} (D^{GDP}, S77L), RagC^{GTP} (C^{GTP}, Q120L), RagC^{GDP} (C^{GDP}, S75L), RagB^{GTP} (B^{GTP}, Q99L), RagB^{GDP} (B^{GDP}, T54L), RagA^{GTP} (A^{GTP}, Q66L), or RagA^{GDP} (A^{GDP}, T21L) was transfected into SW620 cells. HA-tagged proteins were immunoprecipitated and then the precipitated proteins were analyzed by immunoblotting with the indicated antibodies. (*D* and *E*) Effect of LRS, Sestrin2, or EPRS knockdown (*D*) and effect of LRS, Sestrin2, or EPRS overexpression (*E*) on Rag GTPases and S6K phosphorylation. (*F* and *G*) DOX-inducible LRS SW620 cells were untreated (Con) or treated with DOX (LRS). Cells were incubated with 20 μM BC-LI-0186 for 90 min and then deprived of BC-LI-0186 for the indicated times. Relative intensity of GTP-loaded RagD (RagD^{GTP}) (*F*) or GTP-loaded RagB (RagB^{GTP}) (*G*) in *SI Appendix*, Fig. S2*D* was normalized to ARF1 and quantified with respect to 0 min. (*H* and *I*) DOX-inducible sh-LRS SW620 cells were untreated (Con) or treated with DOX (sh-LRS). Relative intensity of RagD^{GTP} (*H*) or RagB^{GTP} (*I*) in *SI Appendix*, Fig. S2*E* was quantified. (*J* and *K*) SW620 cells were transfected with control or Sestrin2 cDNA for 24 h. Relative intensity of RagD^{GTP} (*J*) or RagB^{GTP} (*K*) in *SI Appendix*, Fig. S2*F* was quantified. (*L* and *M*) SW620 cells were transfected with control or Sestrin1/2 siRNA, incubated with 20 μM BC-LI-0186 for 90 min, and then deprived of BC-LI-0186 for the indicated times. Relative intensity of RagD^{GTP} (*L*) or RagB^{GTP} (*M*) in *SI Appendix*, Fig. S2*G* was quantified.

the conversion of the RagD–RagB than the RagC–RagA pair (Fig. 3 *A* and *B* and *SI Appendix*, Fig. S3 *A* and *B*). The effects of inactive (RagD^{GTP}–RagB^{GDP}), intermediate (RagD^{GDP}–RagB^{GDP}), and active (RagD^{GDP}–RagB^{GTP}) pairs on S6K phosphorylation further confirmed this kinetic model (Fig. 3*F*). Glutamine levels affected the GTP status of ARF1 but not Rag GTPases (Fig. 3 *G* and *H* and *SI Appendix*, Fig. S3 *E* and *F*), and arginine levels did not affect the GTP levels of Rag GTPases and ARF1 (Fig. 3 *I* and *J* and *SI Appendix*, Fig. S3 *G* and *H*). These results suggest that GTP hydrolysis of RagD plays an initiating role in mTORC1 activation while the RagB–RagD pair functions as a "commencer" of the Rag GTPase cycle during leucine signaling.

Initiating Role of the RagD–RagB Heterodimer in Leucine Signaling. To determine the differential roles of Rag GTPase heterodimers, we investigated the preference of heterodimer formation among endogenous Rag GTPases. In immunoprecipitation assays, endogenous and exogenous RagD preferentially formed a complex with RagB whereas endogenous and exogenous RagC interacted with RagA (Fig. 4*A* and *SI Appendix*, Fig. S4 *A* and *B*). Likewise, endogenous RagB and RagA preferentially interacted with RagD and RagC, respectively (Fig. 4*B*). Interestingly, LRS specifically interacted with the RagD–RagB, but not the RagC–RagA, heterodimer, consistent with a previous report showing LRS as a RagD-GAP (13). In addition, the Ragulator complex component LAMTOR2 showed higher affinity to the RagD–RagB heterodimer than to the RagC–RagA heterodimer (Fig. 4 *A* and *B*).

To further confirm the dominant role of the RagD–RagB heterodimer in leucine signaling, we suppressed each Rag GTPase and determined its effect on the entire Rag GTPase cycle, as well as S6K phosphorylation. RagD knockdown inhibited the leucine-dependent change of all of the other Rag GTPases, whereas knockdown of the other Rag GTPases affected only their corresponding partners (Fig. 4*C*). Ectopic introduction of RagD^{GTP} or the RagD^{GDP} mutant induced the conversion of all Rag GTPases, whereas RagC^{GTP} or RagC^{GDP} influenced only its corresponding partner, RagA (Fig. 4*D*). Overexpression of RagB or RagA mutants affected only their corresponding pairs (Fig. 4*E*). Since LRS functions as a RagD-GAP (13), we investigated how LRS knockdown or BC-LI-0186, which is a specific inhibitor for LRS–RagD binding (15), would influence the entire Rag GTPase cycle. LRS knockdown by doxycycline (DOX)-inducible sh-LRS or BC-LI-0186 treatment decreased leucine-induced RagB^{GTP} and

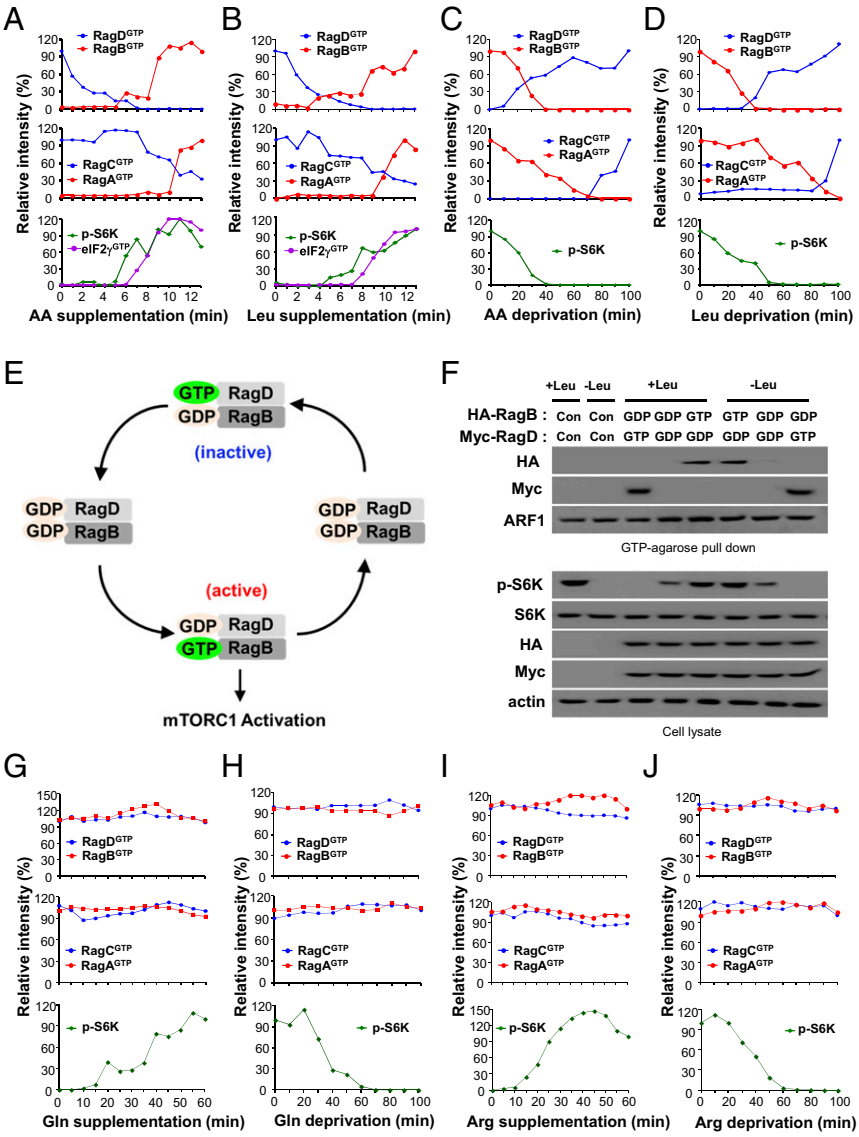

Fig. 3. Kinetics of the Rag GTPase cycle in amino acid signaling. (*A* and *B*) SW620 cells were starved of amino acids (*A*) or leucine (*B*) for 90 min and restimulated with amino acids or leucine for 13 min. Relative intensities of $RagD^{GTP}$, $RagB^{GTP}$, $RagC^{GTP}$, $RagA^{GTP}$, and p-S6K in *SI Appendix*, Fig. S3 *A* and *B* are shown. (*C* and *D*) SW620 cells were starved of amino acids (*C*) or leucine (*D*) for 100 min. Relative intensities of $RagD^{GTP}$, $RagB^{GTP}$, $RagC^{GTP}$, $RagA^{GTP}$, and p-S6K in *SI Appendix*, Fig. S3 *C* and *D* are shown. (*E*) Schematic representation for the kinetic model of the RagD–RagB GTPase cycle during leucine signaling. (*F*) Effects of an inactive ($RagD^{GTP}$–$RagB^{GDP}$), intermediate ($RagD^{GDP}$–$RagB^{GDP}$), or active ($RagD^{GDP}$–$RagB^{GTP}$) pair on Rag GTPases and S6K phosphorylation. (*G* and *H*) SW620 cells were starved of glutamine for 100 min and restimulated with glutamine for 60 min (*G*) or starved of glutamine for 100 min (*H*). Relative intensities of $RagD^{GTP}$, $RagB^{GTP}$, $RagC^{GTP}$, $RagA^{GTP}$, and p-S6K in *SI Appendix*, Fig. S3 *E* and *F* are shown. (*I* and *J*) SW620 cells were starved of arginine for 100 min and restimulated with arginine for 60 min (*I*) or starved of arginine for 100 min (*J*). Relative intensities of $RagD^{GTP}$, $RagB^{GTP}$, $RagC^{GTP}$, $RagA^{GTP}$, and p-S6K in *SI Appendix*, Fig. S3 *G* and *H* are shown.

$RagA^{GTP}$ while increasing $RagD^{GTP}$ and $RagC^{GTP}$, even in the absence of leucine, resulting in S6K dephosphorylation (Fig. 4 *F* and *G*). These data further confirmed the functional importance of RagD (controlled by LRS) in regulating the entire Rag GTPase cycle.

Next, we introduced either the $RagD^{WT}$–$RagB^{WT}$ or $RagC^{WT}$–$RagA^{WT}$ pairs and determined their effects on S6K phosphorylation. Earlier and stronger S6K phosphorylation was observed upon $RagD^{WT}$–$RagB^{WT}$ supplementation (Fig. 4 *H* and *I* and *SI Appendix*, Fig. S4 *C* and *D*). Ectopic supplementation of the active $RagD^{GDP}$–$RagB^{GTP}$ heterodimer restored S6K phosphorylation that was suppressed by RagA/C knockdown, but the converse was not observed (Fig. 4*J*). Active $RagD^{GDP}$–$RagB^{GTP}$, but not $RagC^{GDP}$–$RagA^{GTP}$, also restored S6K phosphorylation in the LRS knockdown cells (Fig. 4*K*). Overexpression of the inactive $RagD^{GTP}$–$RagB^{GDP}$ heterodimer suppressed LRS-mediated S6K phosphorylation (Fig. 4*L*). Overexpression of $RagD^{GDP}$, but not $RagC^{GDP}$, restored S6K phosphorylation that was suppressed by RagC or RagD knockdown (*SI Appendix*, Fig. S4*E*). Furthermore, overexpression of $RagB^{GTP}$, but not $RagA^{GTP}$, restored S6K phosphorylation that was suppressed by RagA or RagB knockdown (*SI Appendix*, Fig. S4*F*). All of these results suggest the initiating and dominant role of RagD–RagB over the RagC–RagA heterodimer in mTORC1 activation.

Coordination of the Rag GTPase Cycle by LRS and Sestrin2. We examined the functional relationship between LRS and Sestrin2 in the Rag GTPase cycle. First, we found that LRS overexpression accelerated (Fig. 5 *A* and *B*), whereas LRS knockdown decelerated, the changes in $RagD^{GTP}$ and $RagB^{GTP}$ (Fig. 5 *C* and *D*). In contrast, Sestrin1/2 knockdown accelerated (Fig. 5 *A* and *C*), whereas Sestrin2 overexpression suppressed, GTP binding of RagB without any change in $RagD^{GTP}$ (Fig. 5 *B* and *D*), further supporting the notion that LRS and Sestrin2 have distinct roles in regulating the Rag GTPase cycle. LRS overexpression enhanced S6K phosphorylation (Fig. 5 *A* and *B*) and cell growth (Fig. 5*E*) regardless of leucine and Sestrin2 levels. Conversely, LRS knockdown inhibited S6K phosphorylation (Fig. 5 *C* and *D*), cell growth (Fig. 5*F*), and cell size (Fig. 5*G*), even in the presence of leucine and Sestrin2, supporting the functional significance of LRS in the leucine-dependent Rag GTPase–mTORC1 axis. Interestingly, Sestrin1/2 knockdown induced $RagB^{GTP}$ formation, S6K phosphorylation (Fig. 5 *A* and *D*), and cell growth (Fig. 5*F*) and enlarged cell size (Fig. 5*G*) even though LRS was suppressed, implying its importance as a negative

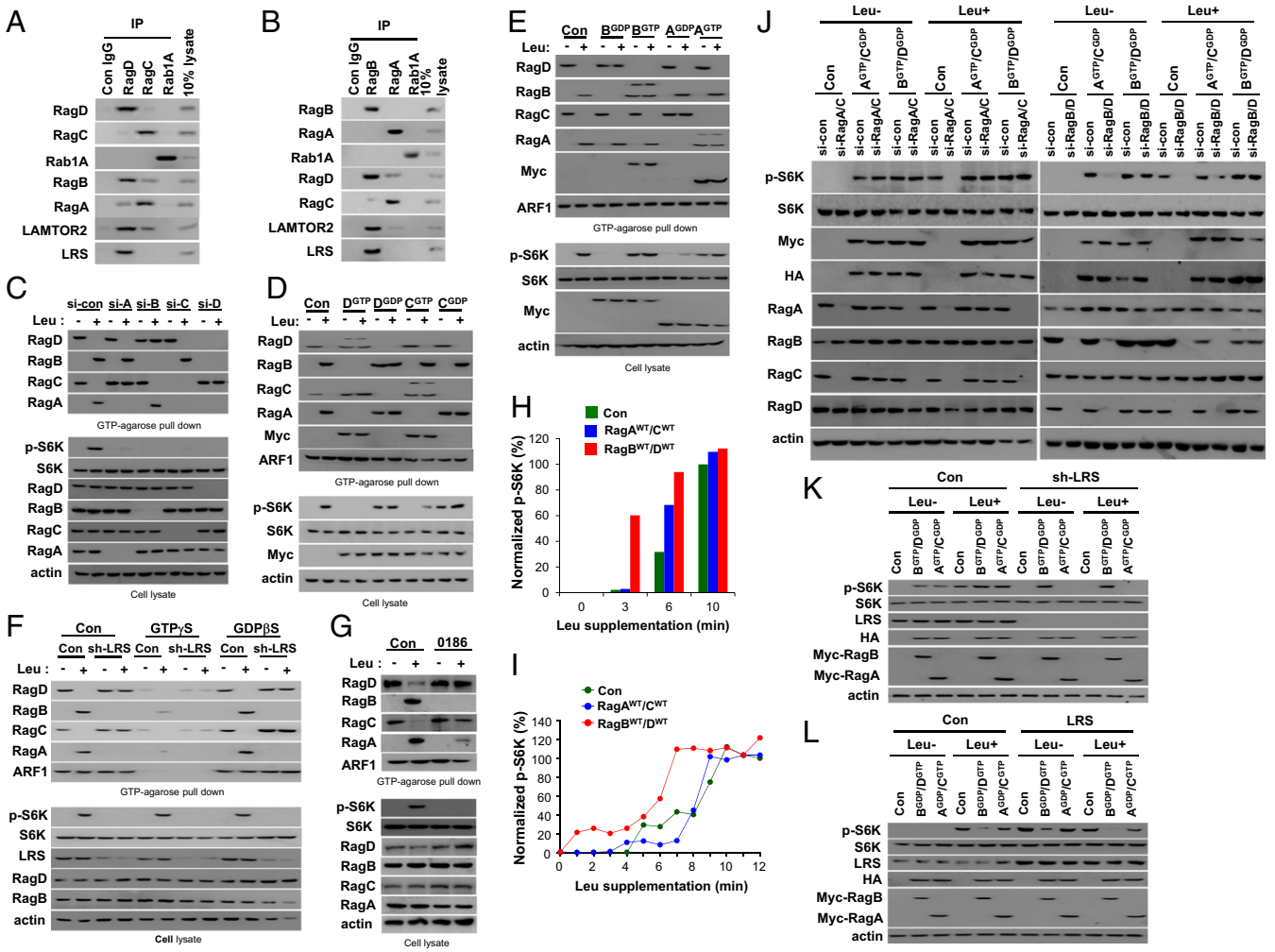

Fig. 4. Dominant role of the RagD–RagB heterodimer in leucine signaling. (*A* and *B*) Interaction of endogenous RagD with RagB. SW620 cell lysates were subjected to immunoprecipitation with anti-RagD, -RagC, or -Rab1A antibodies (*A*) or with anti-RagB, -RagA, or -Rab1A antibodies (*B*). Coimmunoprecipitation was confirmed by immunoblotting with the indicated antibodies. (*C*) SW620 cells transfected with control or siRNA against RagA, B, C, or D were starved of leucine for 90 min and restimulated for 10 min. The proteins precipitated with GTP-conjugated agarose beads were analyzed by immunoblotting with the indicated antibodies. (*D* and *E*) SW620 cells were transfected with Myc-RagD^{GTP}, Myc-RagD^{GDP}, Myc-RagC^{GTP}, or Myc-RagC^{GDP} (*D*) or with Myc-RagB^{GTP}, Myc-RagB^{GDP}, Myc-RagA^{GTP}, or Myc-RagA^{GDP} (*E*). The proteins precipitated with GTP-conjugated agarose beads were analyzed by immunoblotting with the indicated antibodies. (*F*) Dox-inducible sh-LRS SW620 cells were untreated (Con) or treated with DOX (sh-LRS). Cells were starved of leucine for 90 min and restimulated with leucine for 10 min. Cell lysates were incubated with GTP-conjugated agarose beads in the presence of 100 μM GTPγS or GDPβS. (*G*) Effect of BC-LI-0186 on the leucine-induced change of Rag GTPases. Cells were treated with 20 μM BC-LI-0186 for 1 h and then cell lysates were incubated with GTP-conjugated agarose beads, and the precipitated proteins were analyzed by immunoblotting with the indicated antibodies. (*H* and *I*) Dominant effect of the RagD–RagB pair on S6K phosphorylation. Normalized protein intensity graph of *SI Appendix*, Fig. S4*C* (*H*) or *SI Appendix*, Fig. S4*D* (*I*). Phosphorylated S6K was normalized to total S6K and quantified with respect to 10 or 12 min of the control group, respectively. (*J*) SW620 cells were transfected with si-RagA/si-RagC or si-RagD/si-RagB. After 24 h, cells were retransfected with active Rag GTPase (Myc-RagC^{GDP}–HA-RagA^{GTP} or Myc-RagD^{GDP}–HA-RagB^{GTP}). Cells were starved of leucine for 90 min and restimulated for 10 min. Cell lysates were immunoblotted with the indicated antibodies. (*K* and *L*) SW620 cells harboring Dox-inducible sh-LRS (*K*) or LRS (*L*) were untreated (Con) or treated with DOX. Cells were transfected with active Rag GTPase (Myc-RagD^{GDP}–HA-RagB^{GTP} or Myc-RagC^{GDP}–HA-RagA^{GTP}) (*K*) or inactive Rag GTPase (Myc-RagD^{GTP}–HA-RagB^{GDP} or Myc-RagC^{GTP}–HA-RagA^{GDP}) (*L*). Cells were starved of leucine for 90 min and restimulated for 10 min. Cell lysates were analyzed with the indicated antibodies.

regulator of the Rag GTPase cycle. These results demonstrate that LRS-regulated GTP hydrolysis of RagD is an initiating controller of the Rag GTPase cycle during leucine signaling, whereas Sestrin2-regulated GTP hydrolysis of RagB terminates the Rag GTPase cycle.

Ragulator Mediation of the Interplay Between LRS and Sestrin2 for the Rag GTPase Cycle. Since the Ragulator complex functions as a GEF for RagA–RagB (24), knockdown of LAMTOR2, a component of the Ragulator complex, inhibited leucine-induced RagB^{GTP} formation and S6K phosphorylation, thereby "freezing" the Rag GTPase cycle (Fig. 6*A*). To confirm our model of the Rag GTPase cycle, we investigated the functional relationship of the Ragulator complex with LRS and Sestrin2. Interestingly, LAMTOR2 knockdown offset the effects of LRS overexpression (Fig. 6*A*), RagD^{GDP} overexpression (Fig. 6*B*), Sestrin1/2 knockdown (Fig. 6*C*), and the combination of LRS overexpression and Sestrin1/2 knockdown (Fig. 6*D*) on RagB^{GTP} formation and S6K phosphorylation. This effect was diminished by RagB^{GTP} overexpression. These results suggest that the GTP formation of RagB, controlled by Ragulator, is critical for the interplay between LRS and Sestrin2 for the Rag GTPase cycle and mTORC1 activation. Based on our results, we have added LRS, Ragulator, and Sestrin2 to the kinetic model of the

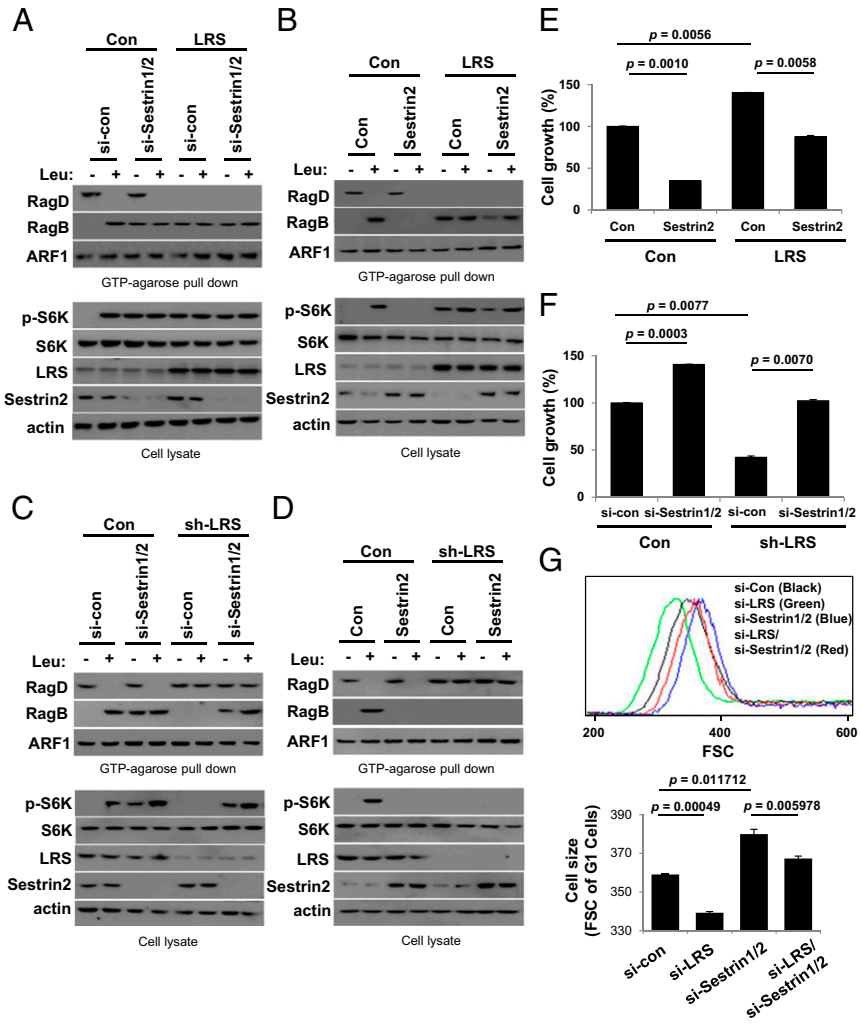

Fig. 5. Coordination of Rag GTPase by LRS and Sestrin2. (*A* and *B*) SW620 cells with inducible LRS overexpression were untreated (Con) or treated with DOX (LRS) and transfected with control or Sestrin1/2 siRNA (*A*) or with control or Sestrin2 cDNA (*B*). Cells were then starved of leucine for 90 min and restimulated with leucine for 10 min. The proteins precipitated with GTP-conjugated agarose beads were analyzed by immunoblotting with the indicated antibodies. (*C* and *D*) SW620 cells with inducible LRS shRNA were untreated (Con) or treated with DOX (sh-LRS) and transfected with control or Sestrin1/2 siRNA (*C*) or with control or Sestrin2 cDNA (*D*). Cells were then starved of leucine for 90 min and restimulated with leucine for 10 min. The proteins precipitated with GTP-conjugated agarose beads were analyzed by immunoblotting with the indicated antibodies. (*E*) Effect of LRS and Sestrin2 overexpression on cell growth. SW620 cells with inducible LRS overexpression were untreated (Con) or treated with DOX (LRS) and transfected with control or Sestrin2 cDNA. Cell growth was quantified and displayed as bar graphs. The error bars represent mean ± SD ($n = 3$). (*F*) Effect of LRS and Sestrin2 knockdown on cell growth. SW620 cells with inducible LRS knockdown were untreated (Con) or treated with DOX (sh-LRS) and transfected with control or Sestrin1/2 siRNA. Cell growth was quantified and displayed as bar graphs. The error bars represent mean ± SD ($n = 3$). (*G*) Size distributions of cells transfected with control, si-LRS, si-Sestrin1/2, or a combination of si-LRS and si-Sestrin1/2. Representative data from three independent experiments (*Upper*). Cell size distributions (Forward scatter-FSC of G1 cells) were quantified (*Lower*). The error bars represent mean ± SD ($n = 3$).

Rag GTPase cycle (Fig. 3*E*) and constructed a coordination model (Fig. 6*E*).

GATOR Complexes Mediate Rag GTPase Regulation by Sestrin2. Since Sestrin2 controls, via GATOR2, the GAP activity of GATOR1 against RagB (16, 22, 23), we next monitored the roles of GATOR1 and GATOR2 in the control of the Rag GTPase cycle. Knockdown of DEPDC5, a component of GATOR1, increased $RagB^{GTP}$ formation and S6K phosphorylation with no effect on the GTP hydrolysis of RagD (Fig. 7*A*). The decrease of $RagB^{GTP}$ and S6K phosphorylation induced by Sestrin2 overexpression was recovered by DEPDC5 knockdown (Fig. 7*A*). However, the elevated $RagB^{GTP}$ induced by DEPDC5 knockdown was unaffected by Sestrin1/2 knockdown (Fig. 7*B*). Sestrin2 overexpression and the knockdown of WDR24, a component of GATOR2, decreased $RagB^{GTP}$ formation and S6K phosphorylation (Fig. 7*C*). The elevated $RagB^{GTP}$ induced by Sestrin1/2 knockdown was reduced by further knockdown of WDR24, suggesting it enhanced GATOR1 activity against RagB (Fig. 7*D*). These results indicate that GATOR1 and GATOR2 mediate the inhibitory effect of Sestrin2 on $RagB^{GTP}$ formation and mTORC1 activation.

Next, we monitored the relationship between LRS (RagD-GAP) and GATOR1 (RagB-GAP) in the control of the Rag GTPase cycle. The combination of LRS overexpression and DEPDC5 knockdown further activated mTORC1 by elevating levels of $RagD^{GDP}$–$RagB^{GTP}$ (Fig. 7*E*). Next, we determined the relationship between LRS and GATOR2 in the control of the Rag GTPase cycle. The decrease in $RagB^{GTP}$ and S6K phosphorylation induced by WDR24 knockdown was recovered by LRS overexpression (Fig. 7*F*). Consistent with the effect on S6K phosphorylation, LRS overexpression enhanced cancer cell growth. This effect was reduced by LAMTOR2 knockdown but not Sestrin1/2 or DEPDC5

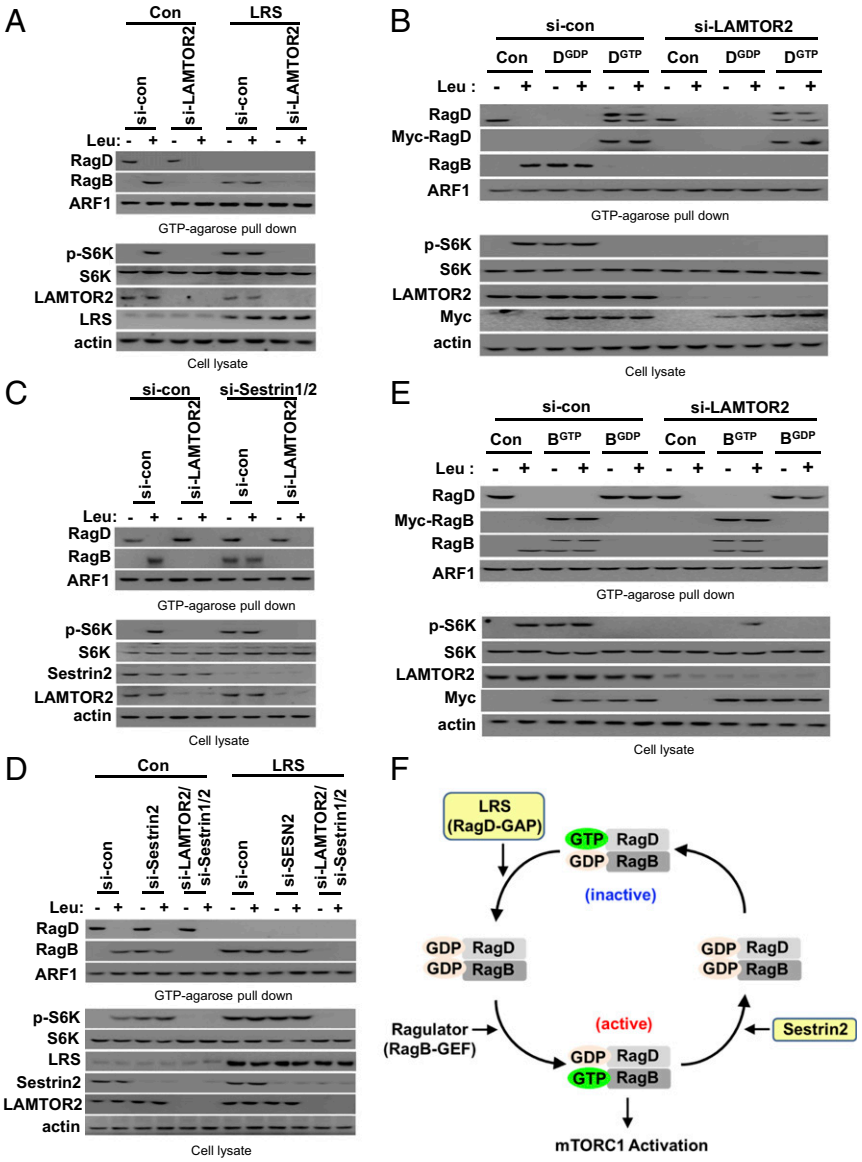

Fig. 6. Ragulator mediation of the interplay between LRS and Sestrin2 in the Rag GTPase cycle. (*A*) The effect of Ragulator knockdown on Rag GTPases and S6K phosphorylation was compared in LRS-normal (Con) and -high (LRS) SW620 cells. SW620 cells with inducible LRS overexpression were untreated (Con) or treated with DOX (LRS) and transfected with control or LAMTOR2 siRNA. Cells were then starved of leucine for 90 min and restimulated with leucine for 10 min. The proteins precipitated with GTP-conjugated agarose beads were analyzed by immunoblotting with the indicated antibodies. (*B*) SW620 cells were transfected with si-control (si-con) or si-LAMTOR2 in combination with control (Con), Myc-RagD^{GDP}, or Myc-RagD^{GTP}. Cells were starved of leucine for 90 min and restimulated with leucine for 10 min. The proteins precipitated with GTP-conjugated agarose beads were analyzed by immunoblotting with the indicated antibodies. (*C*) The effect of Ragulator knockdown on Rag GTPases and S6K phosphorylation was compared in si-control (si-con) or si-Sestrin1/2–transfected SW620 cells. (*D*) The effect of LAMTOR2 knockdown and Sestrin1/2 knockdown on Rag GTPases and S6K phosphorylation were compared in LRS-normal (Con) and -high (LRS) SW620 cells. SW620 cells with inducible LRS overexpression were untreated (Con) or treated with DOX (LRS) and transfected with si-control, si-LAMTOR2, or si-Sestrin1/2 and si-LAMTOR2. Then, cells were starved of leucine for 90 min and restimulated with leucine for 10 min. The proteins precipitated with GTP-conjugated agarose beads were analyzed by immunoblotting with the indicated antibodies. (*E*) SW620 cells were transfected with si-control (si-con) or si-LAMTOR2 in combination with control (Con), Myc-RagB^{GTP}, or Myc-RagB^{GDP}. Cells were starved of leucine for 90 min and restimulated with leucine for 10 min. The proteins precipitated with GTP-conjugated agarose beads were analyzed by immunoblotting with the indicated antibodies. (*F*) Schematic representation for the coordination model of the Rag GTPase cycle by LRS, Ragulator, and Sestrin2.

knockdown (Fig. 7*G*). These results support our coordination model of the Rag GTPase cycle, indicating that LRS is a RagD-GAP that initiates the Rag GTPase cycle; Ragulator is a RagB-GEF, that activates mTORC1; and Sestrin2 controls the RagB-GAP activity of GATOR1 via GATOR2 inhibition, which terminates the Rag GTPase cycle (Fig. 7*H*).

Discussion

Amino acid signaling is a mitogenic pathway that controls growth and metabolic processes (1, 2). Although leucine is known to be the most effective amino acid for mTORC1 activation, glutamine and arginine can also activate mTORC1 via independent routes (27, 30). Our results unveiled a unique position of LRS in the control of the RagD–mTORC1 axis. Although LRS and Sestrin2 share a common role in the mediation of leucine signal for mTORC1 activation, their working mechanisms in the Rag GTPase cycle are idiosyncratic. Perhaps multiple leucine sensors are required for fine control of Rag GTPases in response to different nutritional environments. Whereas LRS is a positive regulator of the Rag GTPase cycle by functioning as a GAP for RagD, Sestrin2 is a negative regulator of the Rag GTPase cycle by inhibiting GATOR2. Thus, LRS and Sestrin2 could work as "on" and "off" switches, respectively, throughout the entire Rag GTPase cycle (Fig. 7*H*). Namely, during leucine signaling, LRS initiates the Rag GTPase cycle via RagD whereas Sestrin2 terminates the Rag GTPase cycle by controlling RagA–RagB GAP activity of GATOR1 via GATOR2 inhibition. Since the K_m value of LRS for leucine in the amino acid activation reaction and the K_d of leucine for Sestrin2 are similar (22, 31), whether LRS and Sestrin2 regulate Rag GTPases independently or cooperatively needs further investigation.

This work also unveiled the kinetic difference and functional hierarchy among Rag GTPases. Interestingly, RagD seems to be functionally dominant among the four Rag GTPases (Fig. 4 *C* and *D*). Since the kinetics of S6K phosphorylation is well-correlated with that of RagB^{GTP} (Fig. 3 *A*–*D*), the GTP–GDP status of RagB seems to be directly involved in mTORC1 activation. The Rag heterodimer that contains RagB^{GTP} directly interacts with Raptor of mTORC1 (6). The GTP–GDP status is rate-limiting for RagB-mediated mTORC1 activation (7). In addition, our results support the notion that GTP hydrolysis of RagD by LRS is critical for leucine-induced RagB^{GTP} formation (Fig. 4 *C* and *D*), which may explain the differential role of RagD and RagB in the Rag heterodimer. LRS-mediated GTP hydrolysis of RagD may control

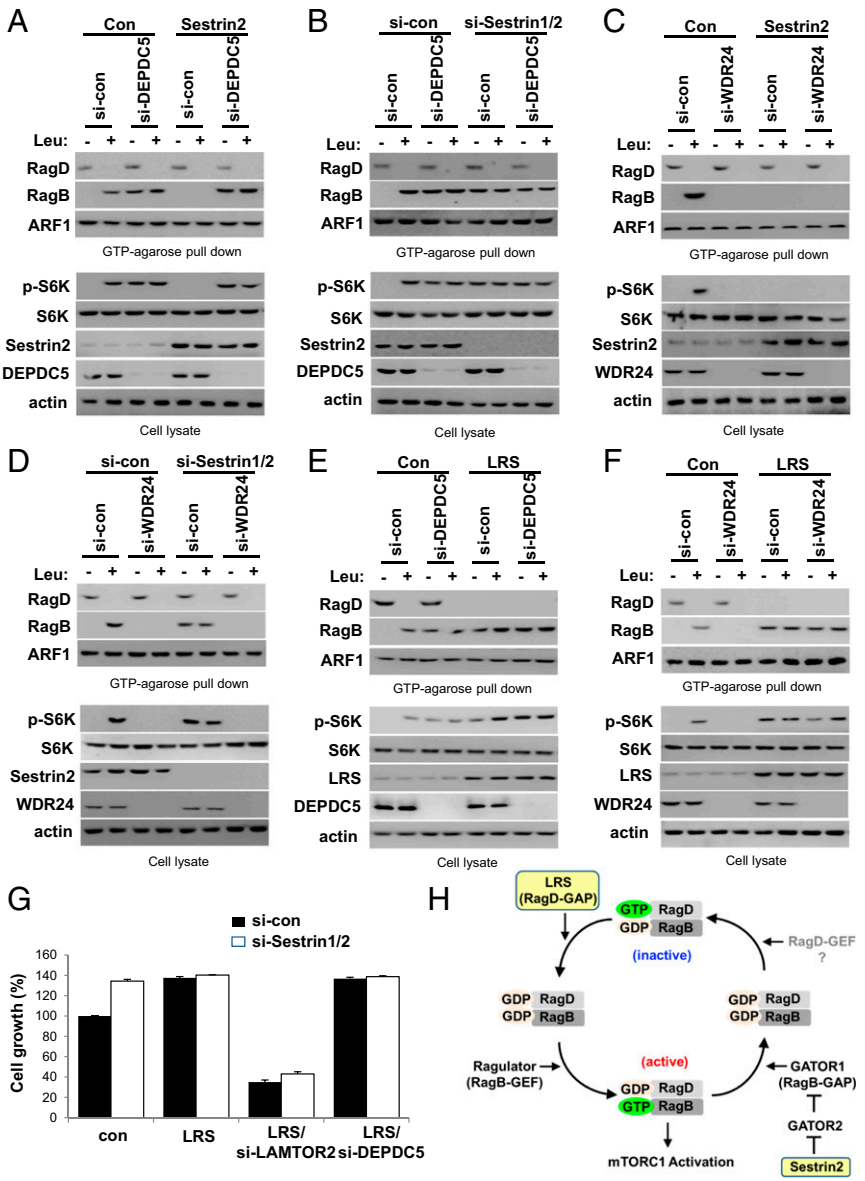

Fig. 7. GATOR complexes mediate Rag GTPase regulation by Sestrin2. (*A*) The effect of GATOR1 knockdown on Rag GTPases and S6K phosphorylation was compared in control (Con) or Sestrin2-transfected SW620 cells. SW620 cells transfected with si-DEPDC5 and Sestrin2 were starved of leucine for 90 min and restimulated with leucine for 10 min. The proteins precipitated with GTP-conjugated agarose beads were analyzed by immunoblotting with the indicated antibodies. (*B*) The effect of GATOR1 knockdown on Rag GTPases and S6K phosphorylation was compared in si-control (si-con) or si-Sestrin1/2–transfected SW620 cells. SW620 cells transfected with si-DEPDC5 and si-Sestrin1/2 were starved of leucine for 90 min and restimulated with leucine for 10 min. The proteins precipitated with GTP-conjugated agarose beads were analyzed by immunoblotting with the indicated antibodies. (*C*) The effect of GATOR2 knockdown on Rag GTPases and S6K phosphorylation was compared in control (Con) or Sestrin2-transfected SW620 cells. SW620 cells transfected with si-WDR24 and Sestrin2 were starved of leucine for 90 min and restimulated with leucine for 10 min. The proteins precipitated with GTP-conjugated agarose beads were analyzed by immunoblotting with the indicated antibodies. (*D*) The effect of GATOR2 knockdown on Rag GTPases and S6K phosphorylation was compared in control (si-con) or si-Sestrin1/2–transfected SW620 cells. SW620 cells transfected with si-WDR24 and si-Sestrin1/2 were starved of leucine for 90 min and restimulated with leucine for 10 min. The proteins precipitated with GTP-conjugated agarose beads were analyzed by immunoblotting with the indicated antibodies. (*E*) The effect of GATOR1 knockdown on Rag GTPases and S6K phosphorylation was compared in LRS-normal (Con) and -high (LRS) SW620 cells. SW620 cells with inducible LRS overexpression were untreated (Con) or treated with DOX (LRS) and transfected with si-DEPDC5. Cells were then starved of leucine for 90 min and restimulated with leucine for 10 min. The proteins precipitated with GTP-conjugated agarose beads were analyzed by immunoblotting with the indicated antibodies. (*F*) The effect of GATOR2 knockdown on Rag GTPases and S6K phosphorylation was compared in LRS-normal (Con) and -high (LRS) SW620 cells. SW620 cells with inducible LRS overexpression were untreated (Con) or treated with DOX (LRS) and transfected with si-WDR24. Cells were then starved of leucine for 90 min and restimulated with leucine for 10 min. The proteins precipitated with GTP-conjugated agarose beads were analyzed by immunoblotting with the indicated antibodies. (*G*) The effects of the knockdown of Sestrin1/2, LAMTOR2, or DEPDC5 on cell growth were compared in LRS-normal (Con) and -high (LRS) SW620 cells. The error bars represent mean ± SD ($n = 3$). (*H*) Proposed model for the Rag GTPase cycle controlled by LRS, Ragulator, and the Sestrin2–GATOR2–GATOR1 pathway during leucine signaling.

GTP loading of RagB via the recruitment of Ragulator, which is a RagB-GEF, leading to a direct interaction of GTP-loaded RagB with Raptor, thereby activating mTORC1.

The entire Rag GTPase cycle is affected by knockdown of LRS and RagD (Fig. 4 *C* and *F*) or overexpression of $RagD^{GDP}$ (Fig. 4*D*), which is possible because the Ragulator complex binds to RagA as well as RagB (Fig. 2*C*), albeit with a different binding affinity (Fig. 4 *A* and *B*). Consistent with these data, Ragulator is known to possess GEF activity toward RagA and RagB (24). Perhaps a conformational change induced by GTP hydrolysis of RagD causes a structural change in Ragulator, leading to activation of its GEF activity. Recently, the structure of the Ragulator complex was revealed, showing that the nucleotide binding, or G domain, of the Rag GTPase is distal from the LAMTOR components of the Ragulator complex (32–34). Thus, the driving force of the nucleotide exchange of RagB by Ragulator may require the GTP hydrolysis of RagD.

It is known that LRS is a component of the multi-tRNA synthetase complex (MSC), which serves as a signaling hub for its component enzymes and factors (35). LRS was also shown to interact with Vps34 in a leucine-dependent manner to activate the mTORC1 pathway (36). It is unclear how cellular localization and target interactions of LRS are regulated at this time. By analogy to the behavior of other MSC components such as EPRS, KRS, and AIMPs (37) and considering that the cellular level of LRS is unchanged by leucine concentration, it is speculative that cellular localization and interaction could be specifically controlled by context-dependent posttranslational modifications of MSC-associated LRS. However, we do not exclude the possibility that freely existing LRS could be primarily recruited for leucine-induced mTORC1 activation.

Our results suggest that the RagD–RagB and RagC–RagA heterodimers play differential roles in the process of mTORC1 activation. However, the exact roles of the RagD–RagB and RagC–RagA heterodimers remain unclear. Since amino acid or

leucine supplementation, LRS knockdown, BC-LI-0186 treatment, or $RagD^{GDP}$ overexpression affected the change of all the Rag GTPases (Fig. 4 *D*, *F*, and *G* and *SI Appendix*, Fig. S3 *A* and *B*) and knockdown of RagA or RagC also blocked leucine-induced S6K phosphorylation (Fig. 4*C*), the RagC–RagA and RagD–RagB heterodimers are somehow involved in the mTORC1 activation process. One possibility is that the RagD–RagB heterodimer directly controls lysosomal translocation of mTORC1 while the RagC–RagA heterodimer affects the TSC–Rheb pathway, since there is a high degree of reciprocal interaction between RagC and TSC1 (38). Amino acids induce lysosomal translocation of mTORC1 and allow it to encounter its activator Rheb on the lysosome (11). Therefore, the RagC–RagA heterodimer may control Rheb inhibition by the TSC complex, although its role in the regulation of mTORC1 requires further investigation. This proposed link between the RagC–RagA heterodimer and TSC–Rheb pathway could provide a possible explanation for why mTORC1 activation occurs only when both Rag GTPases and Rheb are active.

Materials and Methods

Materials. Antibodies, siRNAs, and reagents used in this study can be found in *SI Appendix*, Tables S1–S3, respectively.

Cell Culture. Cell lines and culture methods are described in *SI Appendix, Materials and Methods*.

Lentiviral Infection for the Experimental Model. Generation of stable human Tet-on cell lines that express LRS or LRS shRNA was performed as described in *SI Appendix, Materials and Methods*.

Amino Acid or Leucine Starvation and Stimulation of Cells. For amino acid or leucine starvation, cells were incubated in all-amino acid- or leucine-free RPMI for the indicated time after cells were rinsed with amino acid-free RPMI. For restimulation, cells were incubated with all-amino acid- or leucine-containing RPMI for the indicated time.

In Vivo GTPase Assay. In vivo GTPase assay was done as previously described (13).

GTP-Agarose Bead Pull-Down Assay. GTP-agarose pull-down assay was performed as described in *SI Appendix, Materials and Methods*.

Immunoblot Analysis. Immunoblotting was performed as described in *SI Appendix, Materials and Methods*.

Flow Cytometry. Flow cytometry was performed as described in *SI Appendix, Materials and Methods*.

Cell Growth and Viability Assays. Cell growth and viability were assessed by CellPlayer NucLight Red (4476; Essen BioScience) and CellTox Green Cytotoxicity Assay (G8741; Promega) using IncuCyte Zoom (Essen BioScience) as described in *SI Appendix, Materials and Methods*.

Human CRC Tissues and Immunohistochemistry. This study was carried out according to the provisions of the Helsinki Declaration of 1975 and was reviewed and approved by the Institutional Review Board of Severance Hospital (IRB-3-2014-0287) with a waiver of informed consent. Immunohistochemical analysis was performed as described in *SI Appendix, Materials and Methods*.

Oncomine Database. The expression level of *LARS* in cancer and normal cells was analyzed using the Oncomine database (https://www.oncomine.org/resource/login.html) as described in *SI Appendix, Materials and Methods*.

TCGA Database Analysis. The expression level of *LARS* and *MTOR* pathway genes was analyzed using TCGA database (https://cancergenome.nih.gov/) as described in *SI Appendix, Materials and Methods*.

Statistical Analysis. The comparisons of continuous data between groups were performed using analysis of variance, followed by Student's *t* tests.

ACKNOWLEDGMENTS. This work was supported by Global Frontier Project Grants NRF-2013M3A6A4072536 and NRF-M3A6A4-2010-0029785 and by a grant from the Gyeonggi Research Development Program.

1. Bar-Peled L, Sabatini DM (2014) Regulation of mTORC1 by amino acids. *Trends Cell Biol* 24:400–406.
2. González A, Hall MN (2017) Nutrient sensing and TOR signaling in yeast and mammals. *EMBO J* 36:397–408.
3. Powis K, De Virgilio C (2016) Conserved regulators of Rag GTPases orchestrate amino acid-dependent TORC1 signaling. *Cell Discov* 2:15049.
4. Saxton RA, Sabatini DM (2017) mTOR signaling in growth, metabolism, and disease. *Cell* 168:960–976.
5. Dazert E, Hall MN (2011) mTOR signaling in disease. *Curr Opin Cell Biol* 23:744–755.
6. Crino PB (2016) The mTOR signalling cascade: Paving new roads to cure neurological disease. *Nat Rev Neurol* 12:379–392.
7. Sancak Y, et al. (2008) The Rag GTPases bind raptor and mediate amino acid signaling to mTORC1. *Science* 320:1496–1501.
8. Kim E, Goraksha-Hicks P, Li L, Neufeld TP, Guan KL (2008) Regulation of TORC1 by Rag GTPases in nutrient response. *Nat Cell Biol* 10:935–945.
9. Schürmann A, Brauers A, Massmann S, Becker W, Joost HG (1995) Cloning of a novel family of mammalian GTP-binding proteins (RagA, RagBs, RagB1) with remote similarity to the Ras-related GTPases. *J Biol Chem* 270:28982–28988.
10. Sekiguchi T, Hirose E, Nakashima N, Ii M, Nishimoto T (2001) Novel G proteins, Rag C and Rag D, interact with GTP-binding proteins, Rag A and Rag B. *J Biol Chem* 276:7246–7257.
11. Sancak Y, et al. (2010) Ragulator-Rag complex targets mTORC1 to the lysosomal surface and is necessary for its activation by amino acids. *Cell* 141:290–303.
12. Cherfils J, Zeghouf M (2013) Regulation of small GTPases by GEFs, GAPs, and GDIs. *Physiol Rev* 93:269–309.
13. Han JM, et al. (2012) Leucyl-tRNA synthetase is an intracellular leucine sensor for the mTORC1-signaling pathway. *Cell* 149:410–424.
14. Bonfils G, et al. (2012) Leucyl-tRNA synthetase controls TORC1 via the EGO complex. *Mol Cell* 46:105–110.
15. Kim JH, et al. (2017) Control of leucine-dependent mTORC1 pathway through chemical intervention of leucyl-tRNA synthetase and RagD interaction. *Nat Commun* 8:732.
16. Bar-Peled L, et al. (2013) A tumor suppressor complex with GAP activity for the Rag GTPases that signal amino acid sufficiency to mTORC1. *Science* 340:1100–1106.
17. Budanov AV, et al. (2002) Identification of a novel stress-responsive gene Hi95 involved in regulation of cell viability. *Oncogene* 21:6017–6031.
18. Velasco-Miguel S, et al. (1999) PA26, a novel target of the p53 tumor suppressor and member of the GADD family of DNA damage and growth arrest inducible genes. *Oncogene* 18:127–137.
19. Budanov AV, Karin M (2008) p53 target genes sestrin1 and sestrin2 connect genotoxic stress and mTOR signaling. *Cell* 134:451–460.
20. Peng M, Yin N, Li MO (2014) Sestrins function as guanine nucleotide dissociation inhibitors for Rag GTPases to control mTORC1 signaling. *Cell* 159:122–133.
21. Chantranupong L, et al. (2014) The Sestrins interact with GATOR2 to negatively regulate the amino-acid-sensing pathway upstream of mTORC1. *Cell Rep* 9:1–8.
22. Wolfson RL, et al. (2016) Sestrin2 is a leucine sensor for the mTORC1 pathway. *Science* 351:43–48.
23. Kim JS, et al. (2015) Sestrin2 inhibits mTORC1 through modulation of GATOR complexes. *Sci Rep* 5:9502.
24. Bar-Peled L, Schweitzer LD, Zoncu R, Sabatini DM (2012) Ragulator is a GEF for the Rag GTPases that signal amino acid levels to mTORC1. *Cell* 150:1196–1208.
25. Menon S, Manning BD (2008) Common corruption of the mTOR signaling network in human tumors. *Oncogene* 27(Suppl 2):S43–S51.
26. Zoncu R, Efeyan A, Sabatini DM (2011) mTOR: From growth signal integration to cancer, diabetes and ageing. *Nat Rev Mol Cell Biol* 12:21–35.
27. Jewell JL, et al. (2015) Differential regulation of mTORC1 by leucine and glutamine. *Science* 347:194–198.
28. Parmigiani A, et al. (2014) Sestrins inhibit mTORC1 kinase activation through the GATOR complex. *Cell Rep* 9:1281–1291.
29. Jackson RJ, Hellen CUT, Pestova TV (2010) The mechanism of eukaryotic translation initiation and principles of its regulation. *Nat Rev Mol Cell Biol* 11:113–127.
30. Wang S, et al. (2015) Lysosomal amino acid transporter SLC38A9 signals arginine sufficiency to mTORC1. *Science* 347:188–194.
31. Pang YL, Martinis SA (2009) A paradigm shift for the amino acid editing mechanism of human cytoplasmic leucyl-tRNA synthetase. *Biochemistry* 48:8958–8964.
32. de Araujo MEG, et al. (2017) Crystal structure of the human lysosomal mTORC1 scaffold complex and its impact on signaling. *Science* 358:377–381.
33. Yonehara R, et al. (2017) Structural basis for the assembly of the Ragulator-Rag GTPase complex. *Nat Commun* 8:1625.
34. Su MY, et al. (2017) Hybrid structure of the RagA/C-Ragulator mTORC1 activation complex. *Mol Cell* 68:835–846.e3.
35. Kim JH, Han JM, Kim S (2014) Protein-protein interactions and multi-component complexes of aminoacyl-tRNA synthetases. *Top Curr Chem* 344:119–144.
36. Yoon MS, et al. (2016) Leucyl-tRNA synthetase activates Vps34 in amino acid-sensing mTORC1 signaling. *Cell Rep* 16:1510–1517.
37. Guo M, Yang XL (2014) Architecture and metamorphosis. *Top Curr Chem* 344:89–118.
38. Jung J, Genau HM, Behrends C (2015) Amino acid-dependent mTORC1 regulation by the lysosomal membrane protein SLC38A9. *Mol Cell Biol* 35:2479–2494.